

Glass-specific behavior in the damping of acoustic-like vibrations

B. Rufflé,¹ G. Guimbretière,¹ E. Courtens,¹ R. Vacher,¹ and G. Monaco²

¹*Groupe de Physique des Verres et Spectroscopies, LCVN,
UMR 5587 CNRS, Université Montpellier II, F-34095 Montpellier Cedex 5, France*
²*European Synchrotron Radiation Facility, Boîte Postale 220, F-38043 Grenoble, France*

(Dated: May 24, 2019)

High frequency sound is observed in lithium diborate glass, $\text{Li}_2\text{O}-2\text{B}_2\text{O}_3$, using Brillouin scattering of light and x-rays. The sound attenuation exhibits a non-trivial dependence on the wavevector, with a remarkably rapid increase towards a Ioffe-Regel crossover as the frequency approaches the boson peak from below. The analysis of available results on several glasses reveals the near coincidence of the boson-peak frequency with a Ioffe-Regel limit for sound. We conjecture that this behavior is likely to be glass specific and rather universal.

PACS numbers: 63.50.+x, 78.35.+c, 81.05.Kf

The nature of acoustic vibrations in glasses remains a question of considerable interest. Undisputed is that low frequency sound propagates in glasses as in any continuum. Acoustic modes of almost linear dispersion, $\Omega = vq$, are observed over a wide range, *e.g.* up to several hundred GHz in silica [1]. We use Ω for the angular frequency, q for the wavevector, and v for the nearly constant phase velocity of sound. On the low frequency side of this range, ultrasonic damping is generally dominated by relaxing defects [2], rather similar to the situation in defectuous crystals [3]. In the hypersonic regime observed with Brillouin scattering of light, the anharmonicity of atomic vibrations – always important for the temperature dependence of v [4] – also starts affecting the damping [5]. In silica, the anharmonicity should completely dominate the damping at still higher frequencies, near the upper end of the linear dispersion range [5]. Consider now very high acoustic frequencies, those near the end of branches at the zone boundary of crystals. A signature of acousticlike modes was actually observed in silica glass in this range [6]. It appears on the neutron-scattering inelastic structure factor, $S(Q, \omega)$, where ω is the spectral frequency and Q the momentum exchange. Maxima in ω of $S(Q, \omega)$ form pseudo-branches $\Omega(Q)$. The latter are crystal-like, with several broad maxima near zone-edge frequencies and wavevectors following $S(Q)$. This is not really surprising, as in that limit the acoustic vibrations become essentially standing modes in both crystals and glasses. Their frequencies are thus similar, being only sensitive to direct neighbors. The likeliness of very high frequency scattering signals in polycrystals and glasses was also recently reported for a molecular system, ethanol [7].

Between these low and very high frequency ranges, there exists an intermediate acoustic regime where glasses should be very different from crystals, typically around one to a few THz. The phonons responsible for the universal thermal conductivity plateau of glasses fall here [8, 9]. Their wavelength is of the order of a few nanometers, a scale intermediate between short-

range crystal-like structures and the long-range continuum [10, 11]. Their frequency is also near that of the boson peak (BP), a common feature of glasses related to low-lying opticlike modes [12, 13]. Thus the investigation of acousticlike excitations of glasses at frequencies around 1 THz, *i.e.* at energies of a few meV, is of high interest. Scattering experiments in non-periodic systems at these Ω -values and conserving $Q = \Omega/v$ remain difficult. The best inelastic x-ray scattering (IXS) instruments now reach instrumental full-widths down to ~ 1.5 meV with Q -values down to $\sim 1 \text{ nm}^{-1}$ [14]. This allowed observing in permanently densified silica glass, $d\text{-SiO}_2$, the approach from below of a Ioffe-Regel crossover for sound waves [15]. Here, we *define* the crossover position as the angular frequency Ω_{co} where the full-width of sound Γ (in rad/s) reaches Ω_{co}/π . This implies that the energy mean free path ℓ has fallen down to half a wavelength, $\ell \simeq \lambda/2$ [16]. The onset of crossover is characterized by a very rapid increase of Γ with q , up to $q_{\text{co}} \equiv \Omega_{\text{co}}/v$. The choice of $d\text{-SiO}_2$, as opposed to ordinary silica $v\text{-SiO}_2$, was guided by its expected high crossover. We found indeed that $q_{\text{co}} \simeq 2 \text{ nm}^{-1}$, so that the rapid increase of Γ was observed over an order of magnitude, for q increasing from $\sim 1 \text{ nm}^{-1}$ to q_{co} [15]. The present work was motivated by the need to firmly establish a second example of this remarkable behavior. In addition, $d\text{-SiO}_2$ is a technically difficult material, only available in small samples of irregular shapes that lose densification on polishing and whose homogeneity requires careful checking. Such samples are not suitable for many relevant experiments. It is thus of considerable interest to perform decisive scattering measurements around Ω_{co} on an easier to produce glass. The value of Ω_{co} is thought to be related to the position of the BP, Ω_{BP} [17]. We show below that indeed $\Omega_{\text{co}} \simeq \Omega_{\text{BP}}$ for many glasses. A glass compatible with IXS and of high $\hbar\Omega_{\text{BP}} \simeq 9$ meV [18] is lithium diborate, $\text{Li}_2\text{O}-2\text{B}_2\text{O}_3$, or LB2. The existence of a Ioffe-Regel limit in LB2 was already shown in [19]. In this Letter, we present a measurement of the onset of crossover in LB2, together with Brillouin light scattering

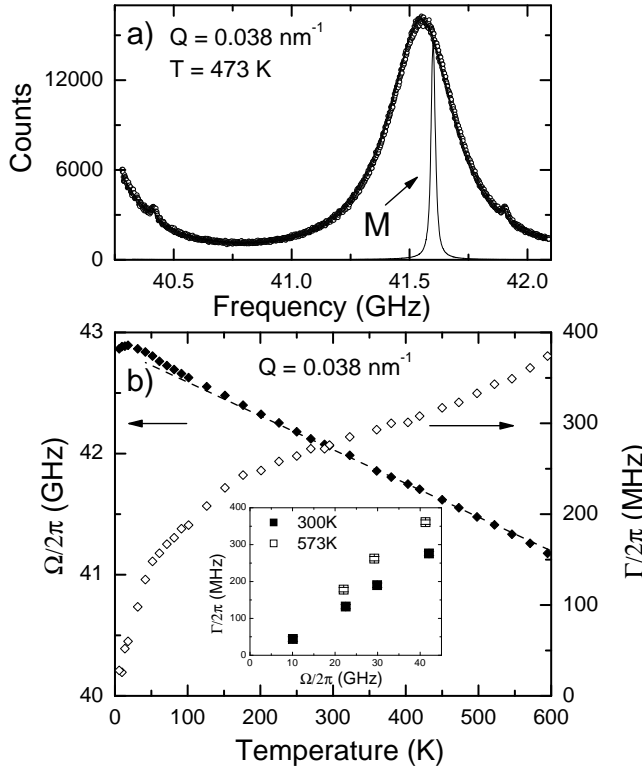


FIG. 1: (a) A typical Brillouin light-scattering spectrum of the LA-mode of LB2 in backscattering ($\theta = 180^\circ$) and its fit to a DHO. The small narrow peaks are produced by the elastic line. Their separation is the free spectral range. M is a reference line showing the instrumental profile. It is obtained by electro-optic modulation of the laser near the Brillouin frequency. (b) The DHO fit parameters *vs* T . The error bars on Ω are much smaller than the symbols, while these on Γ are approximately of that size. This illustrates the extreme precision of the measurement. The dashed line through $\Omega(T)$ corresponds to $\delta\Omega/\Omega \simeq -6.5 \times 10^{-5}T(K)$. The inset shows $\Gamma(\Omega)$ obtained at different scattering angles θ .

(BLS) measurements needed for the interpretation. The results point to the generality of the Ioffe-Regel crossover phenomenon in glasses and to its close connection with the boson peak.

Figure 1 shows BLS results on the longitudinal acoustic (LA) mode of LB2. The spectrum in Fig. 1(a) is excited with an argon-ion laser at 5145 Å, and analyzed with a modern version of a high resolution spectrometer whose principle is described in [20]. The frequencies and linewidths shown in Fig. 1(b) are extracted by adjustment to a damped harmonic oscillator (DHO) lineshape convoluted with the instrumental response, taking into account the broadening due to the finite collection angle. Above ~ 100 K one observes on Ω , or on the relative frequency change $\delta\Omega/\Omega$, a linear decrease in T . Since the scattering vector Q is practically constant, this implies an identical decrease of the relative velocity change, $\delta v/v = -6.5 \times 10^{-5}T(K)$. This behavior is characteris-

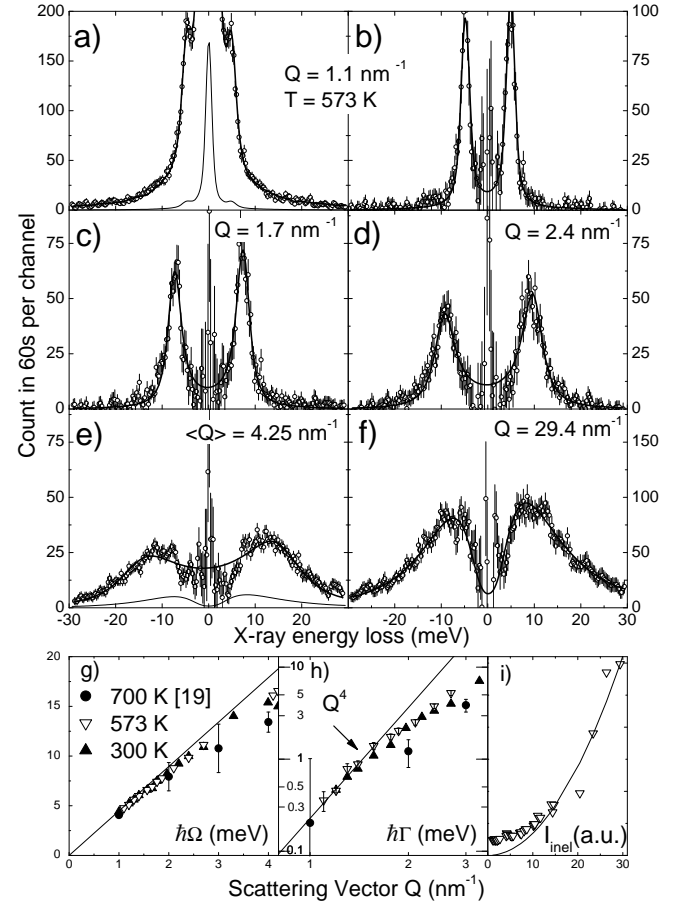


FIG. 2: IXS spectra of LB2 and their fits explained in the text; (a) A full spectrum and its central portion $\times 1/20$; (b-e) DHO fits to the inelastic part after subtraction of the elastic component; (f) A high- Q spectrum reproducing the BP fitted to a log-normal; (g,h) The parameters of the DHO fits for two temperatures; the three full dots are from [19]; the slope of the line in (g) is the velocity from Fig. 1; in (h), the errors bars at 573 K are mostly smaller than the symbols, while these at 300 K (not shown) are about twice as large. The line of slope 4 in (h) is drawn through the first five points at 573 K. (i) The integrated inelastic intensities at 573 K corrected for the oxygen-ion form factor, with a line $\propto Q^2$.

tic of anharmonic coupling of sound to the thermal bath [4]. At these high frequencies, the effect of thermal relaxations on the *velocity* is generally weak and only felt at low temperatures [5], as seen in Fig. 1(b). The matter is quite different for the *damping*. In ultrasound, relaxation produces in LB2 a relatively strong damping, also very broad in T [21]. The damping shown in Fig. 1(b) appears to be still dominated by this relaxation. Indeed, measuring as a function of scattering angle, we find that Γ is approximately proportional to Ω as shown in the inset. This is characteristic of relaxation at frequencies around the maximum in Ω of the internal friction [2].

X-ray Brillouin scattering experiments, illustrated in Fig. 2, were performed on the high-resolution spectrome-

ter ID16 at the European Synchrotron Radiation Facility in Grenoble, France. The experimental conditions were similar to those described in [15]. Measurements were taken at two temperatures, 300 and 573 K. Elevated temperatures are favorable to increase the Brillouin signal by the Bose factor. However, we refrained from nearing the glass transition, as Li^+ diffusion grows then rapidly [22]. Figs. 2(a-f) illustrate typical spectra at 573 K and their fits. The indicated Q -values correspond to the center of the collection slit which gives a spread $\Delta Q \simeq \pm 0.18 \text{ nm}^{-1}$. The spectrum in Fig. 2(a) is taken at the smallest usable Q . It consists of an elastic peak plus a Brillouin doublet. The small constant background, fixed to the known detector noise, is already subtracted. Each such spectrum was adjusted to an elastic line plus a DHO, convoluted with the separately measured instrumental response, taking into account the frequency spread produced by the collection aperture. For clarity, only the inelastic parts of the spectra are shown in Figs. 2(b-f). These are obtained by subtracting the fitted elastic intensity from the data. The apparent Brillouin width in Fig. 2(b) is nearly all instrumental, while it contains an appreciable broadening in Fig. 2(c). The latter becomes the dominant part in Fig. 2(d) for which $Q \simeq q_{\text{co}}$, with $\Omega_{\text{co}} \simeq 9 \text{ meV}$ as shown below. It is seen that the DHO lineshape starts deviating systematically from the measured signal around q_{co} . The spectrum in Fig. 2(e) is actually the mean of four spectra accumulated from 4.1 to 4.4 nm^{-1} . At these high Q -values the spectra evolve so slowly with Q that taking a mean is a good procedure to increase the signal-to-noise ratio. The additional spread in Q was taken into account in the fit which however is then quite poor, showing that the DHO is no more a valid approximation. Fig. 2(f) shows a spectrum at 29.4 nm^{-1} fitted to a log-normal [23]. This is essentially the BP as discussed below.

The parameters extracted from the DHO fits of the IXS spectra are displayed in Figs. 2(g,h). They show little dependence on T . Below the crossover there is only a slight departure from linear dispersion as seen in Fig. 2(g). There is however a very rapid increase of the damping for the smallest Q values shown in Fig. 2(h). A power law Q^4 has been drawn through the five lowest points at 573 K. A fit to these five points actually gives the power 4.2 ± 0.1 . As can be expected, this rapid increase of Γ tends to saturate as the crossover is approached from below, starting at $Q \sim 2 \text{ nm}^{-1}$. There is then a progressive merging of the sound waves with the opticlike BP. The position of opticlike modes is Q -independent, which we observe in comparing spectra taken at 23.4, 26.4, and 29.4 nm^{-1} . In the incoherent approximation, their integrated intensity should be proportional to Q^2 . The total inelastic intensity I_{inel} , corrected for the atomic form factor of oxygen, is shown in Fig. 2(i). At low Q , the Brillouin signal contributes a constant. The Q^2 dependence is seen at high Q , confirming that Fig. 2(f) shows mainly the

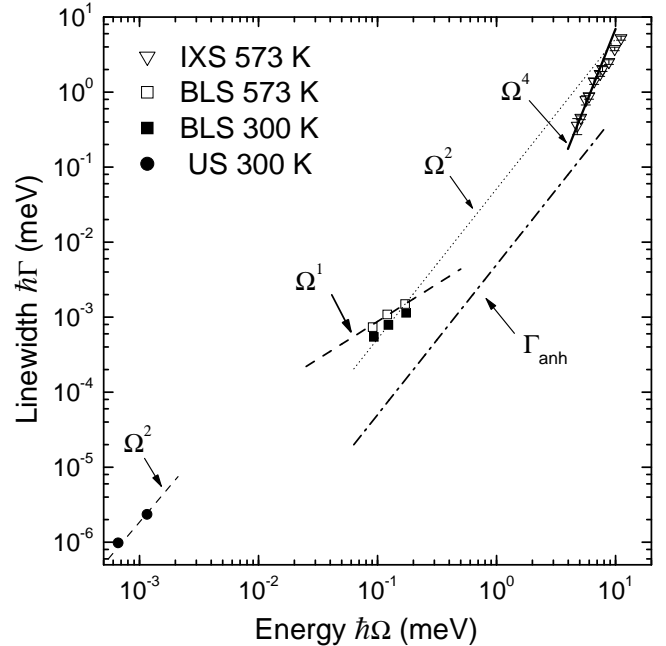


FIG. 3: Overview of $\Gamma(\Omega)$ in different regimes. The lines are guides to the eye discussed in the text.

scattering from the BP, whose shape actually agrees with Raman scattering [18]. Extrapolating the intensity of the log-normal shown in (f) to the Q -value in (e) leads to the thin line drawn there. Hence, what is seen in Figs. 2(b-e) is mostly produced by acousticlike excitations while at higher Q these merge into opticlike modes. A similar merging of the acoustic mode into the BP was observed in $d\text{-SiO}_2$ [24].

Figure 3 summarizes, on the energy scale commonly used in IXS, all the acoustic information available on LB2 up to Ω_{co} . It emphasizes the diversity of broadening mechanisms. At low frequencies, the ultrasonic (US) absorption is close to the regime $\Gamma \propto \Omega^2$, as expected for relaxation [2]. In BLS, relaxation leads to $\Gamma \propto \Omega$, from the inset of Fig. 1(b). Here, a line of slope 1 is drawn through the points at 573 K as a guide to the eye. The anharmonic slope in $\delta v/v$ allows estimating the corresponding contribution to the linewidth, Γ_{anh} . Indeed, as long as $\Omega\tau_{\text{th}} \ll 1$, where τ_{th} is the relaxation time of the thermal bath, one has $\Gamma_{\text{anh}} = A\Omega^2\tau_{\text{th}}$ and $\delta v/v = -A/2$, where A is defined in [5]. LB2 is a hard glass of high Ω_{BP} , just as $d\text{-SiO}_2$. It is reasonable to take as rough estimate $\tau_{\text{th}}(s) \simeq 2 \times 10^{-11}/T(\text{K})$, similar to $d\text{-SiO}_2$ [25]. This gives the dash-dotted line of slope 2 in Fig. 3. It implies that in LB2, contrary to $d\text{-SiO}_2$, anharmonicity would only dominate the damping in a small region around 2 meV. At higher energy, it becomes rapidly masked by the onset of hybridization of the acoustic motions with low-lying optic ones, forming the BP. The dotted line in Ω^2 is only drawn to point out that such an interpolation between light and x-ray Brillouin scattering is not justi-

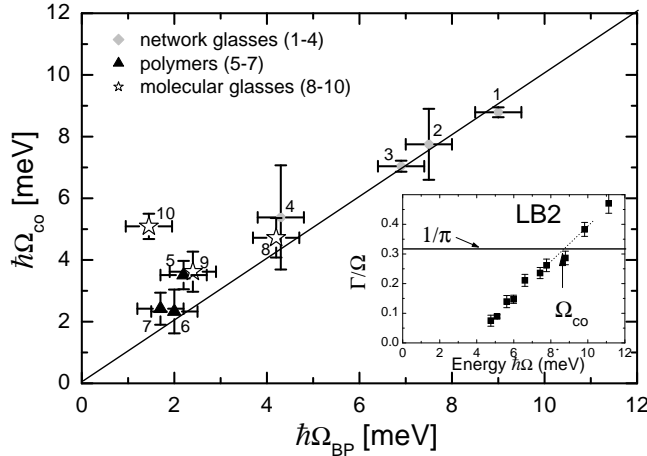


FIG. 4: Ω_{co} vs. Ω_{BP} for various glasses. The line $\Omega_{\text{co}} = \Omega_{\text{BP}}$ is a guide to the eye. The points and the references for $\Gamma(\Omega)$ and Ω_{BP} are: (1) $\text{Li}_2\text{O}-2\text{B}_2\text{O}_3$, here and [18, 19]; (2) $\text{Li}_2\text{O}-4\text{B}_2\text{O}_3$ [18, 19]; (3) $d\text{-SiO}_2$ [15, 24]; (4) $v\text{-SiO}_2$ [13, 26]; (5) polybutadiene [27, 28]; (6) polycarbonate [29]; (7) Se [30, 31]; (8) glycerol [32, 33]; (9) ethanol [7, 34]; (10) OTP [35, 36]. The inset illustrates for LB2 (present data) the method used to determine Ω_{co} .

fied. The Q^2 behavior generally observed near and above crossover might relate to what amounts to a strong inhomogeneous broadening as suggested in [7]. It is meaningless to extrapolate it below the crossover.

The rapid onset of the crossover has now been observed in the two glasses examined in sufficient details, $d\text{-SiO}_2$ and LB2, revealing that $\Omega_{\text{co}} \simeq \Omega_{\text{BP}}$. It is legitimate to ask whether this is a universal property. Analogous considerations were already presented in [17]. The crossover positions were there estimated using the soft-potential model combined with measured two-level-system parameters. The current definition of Ω_{co} now allows to locate it using IXS data, taking the intercept of Γ/Ω with $1/\pi$, as shown in the inset of Fig. 4. For LB2, this gives $\hbar\Omega_{\text{co}} \simeq 9$ meV and $q_{\text{co}} \simeq 2.4 \text{ nm}^{-1}$. Although the onset was not observed in sufficient details by others, there is enough information on several glasses to draw such plots. A summary of this analysis is given in Fig. 4. The vertical error bars result from indeterminations in the published $\Gamma(\Omega)$ data. We kept in Fig. 4 all the glasses for which these errors are reasonably small. The horizontal error bars, the same for all points, is a fair estimate of the inaccuracy of BP ‘positions’. Fig. 4 demonstrates that indeed the crossovers and the BP positions coincide in most cases. Out of ten glasses, only OTP falls significantly off the line, owing to its very low observed BP [36]. However, OTP has many external modes [36]. It is conceivable that the observed BP only corresponds to the crossover for transverse acoustic modes, masking another one for LA modes. This would explain this apparent failure of universality. A physical reason for the universality is that a bilinear coupling of quasilocal oscillators with

the strain field redistributes the density of states of the former, leading to $\Omega_{\text{BP}} = \Omega_{\text{co}}$ [17, 37]. If so, we conjecture that the rapid onset of the crossover should also be a universal property of glasses. That it was not evidenced, for example in $v\text{-SiO}_2$ [26], is explained by the low value of q_{co} in that case. This should be an incentive to further increase the already remarkable performances of IXS instruments.

The authors thank A. Matic and L. Börjesson for the LB2 sample, R. Vialla for improvements to the BLS spectrometer, and J.M. Fromental for technical assistance.

- [1] M. Rothenfusser *et al.*, Phys. Rev. B **27**, R5196 (1983).
- [2] S. Hunklinger and W. Arnold, in *Physical Acoustics*, Vol. XII, W.P. Mason and R.N. Thurston Eds. (Academic Press, New York, 1976), p. 155.
- [3] See *e.g.*, *Physical Acoustics*, Vol. IIIA, W.P. Mason, Ed. (Academic Press, New York, 1966).
- [4] T.N. Claytor *et al.*, Phys. Rev. B **18**, 5842 (1978).
- [5] R. Vacher *et al.*, arXiv:cond-mat/0505560, 23 May 2005.
- [6] M. Arai *et al.*, Physica B **263-264**, 268 (1999).
- [7] A. Matic *et al.*, Phys. Rev. Lett. **93**, 145502 (2004).
- [8] R.C. Zeller and R.O. Pohl, Phys. Rev. B **4**, 2029 (1971).
- [9] J.E. Graebner *et al.*, Phys. Rev. B **34**, 5696 (1986).
- [10] R.L. Mozzi and B.E. Warren, Acta Cryst. **21**, 459 (1966).
- [11] A.M. Levelut and A. Guinier, Bull. Soc. Fr. Minéral. Cristallog. **90**, 445 (1967).
- [12] U. Buchenau *et al.*, Phys. Rev. B **34**, 5665 (1986).
- [13] B. Hehlen *et al.*, Phys. Rev. Lett. **84**, 5355 (2000).
- [14] R. Verbeni *et al.*, J. Synchrotron Rad. **3**, 62 (1996).
- [15] B. Rufflé *et al.*, Phys. Rev. Lett. **90**, 095502 (2003).
- [16] E. Courtens *et al.*, J. Phys.: Condens. Matter **15**, S1279 (2003); this definition needs not give exactly the same value for Ω_{co} as one based on a particular lineshape [see M. Foret *et al.*, Phys. Rev. Lett. **77**, 3831 (1996)].
- [17] D.A. Parshin and C. Laermans, Phys. Rev. B **63**, 132203 (2001).
- [18] J. Lorösch *et al.*, J. Non-Cryst. Solids **69**, 1 (1984).
- [19] A. Matic *et al.*, Phys. Rev. Lett. **86**, 3803 (2001).
- [20] R. Vacher *et al.*, Rev. Sci. Instrum. **51**, 288 (1980).
- [21] D. Čiplys and J.Y. Prieur, J. Physique (Paris) **42**, C6-184 (1981).
- [22] T. Matsuo *et al.*, Solid State Ionics **154-155**, 759 (2002).
- [23] V.K. Malinovsky *et al.*, Europhys. Lett. **11**, 43 (1990).
- [24] M. Foret *et al.*, Phys. Rev. B **66**, 024204 (2002).
- [25] E. Rat *et al.*, arXiv:cond-mat/0505558, 23 May 2005.
- [26] R. Dell’Anna *et al.*, Phys. Rev. Lett. **80**, 1236 (1998).
- [27] D. Fioretto *et al.*, Phys. Rev. E **59**, 4470 (1999).
- [28] U. Buchenau *et al.*, Phys. Rev. Lett. **77**, 4035 (1996).
- [29] J. Mattsson *et al.*, J. Phys.: Condens. Matter **15**, S1259 (2003).
- [30] T. Scopigno *et al.*, Phys. Rev. Lett. **92**, 025503 (2004).
- [31] M. Foret *et al.*, Phys. Rev. Lett. **81**, 2100 (1998).
- [32] F. Sette *et al.*, Science **280**, 1550 (1998).
- [33] J. Wuttke *et al.*, Phys. Rev. E **52**, 4026 (1995).
- [34] M.A. Ramos *et al.*, Phys. Rev. Lett. **78**, 82 (1997).
- [35] G. Monaco *et al.*, Phys. Rev. Lett. **80**, 2161 (1998).
- [36] A. Tölle, Rep. Prog. Phys. **64**, 1473 (2001).
- [37] V.L. Gurevich *et al.*, Phys. Rev. B **67**, 094203 (2003).